

EREM 74/2 Journal of Environmental Research, Engineering and Management Vol. 74 / No. 2 / 2018 pp. 34-51 DOI 10.5755/j01.erem.74.2.20917 © Kaunas University of Technology	Meandering and Land Use/Cover Change Detection in the Lower Jordan River, 1984–2016, Using GIS and RS	
	Received 2018/06	Accepted after revision 2018/09
	 http://dx.doi.org/10.5755/j01.erem.74.2.20917	

Meandering and Land Use/Cover Change Detection in the Lower Jordan River, 1984–2016, Using GIS and RS

Yusra Al-husban

Associate Professor, Department of Geography, Faculty of Arts, University of Jordan, Amman, Jordan

Corresponding author: y.alhusban@ju.edu.jo

Yusra Al-husban, Associate Professor, Department of Geography, Faculty of Arts, University of Jordan, Amman, Jordan

The objective of this study is to monitor and analyze the meandering and changes in land use/land cover (LULC) caused by the large reduction of water flow of the lower Jordan River (LJR), resulting from climatic conditions and conflict over water resources between Syria, Jordan, Israel and the Palestinian Authority in the upper part of the Jordan River Basin. These circumstances have led to dramatic decline in the Dead Sea level by a vertical distance of -39 m during the monitoring period. This has resulted in the scarcity of water resources, changes affecting the geomorphology of the river as well as the vegetated area and the spatial distribution of riparian vegetation in the LJR. These changes were examined using Landsat TM, ETM, all images acquired in August 1984, 2000, and 2016, and a topographic map (TM) was used as a base map. The multi-temporal images were geometrically and radiometrically calibrated to each other and used as input for an automatic change detection procedure. The results of the interpretation showed that there was an elongation in the active channel length of about 741.8 m within the monitoring period as a result of the Dead Sea shoreline retreat, and about 2.65 km caused by meandering. The direction of the migration rates varied towards the west and the east, with the dominant direction towards the west and the annual average migration rate for the west and the east was 0.325 m, with a total lateral migration during the study period about only 17.875m in both directions the west and the

east. River meandering increased from 1.8 m to 2.1 m in the period. With respect to LULC, the difference image indicated that significant positive changes in green vegetation occurred between 1984 and 2016; this is due to the expansion of water storage by canals and dams in all riparian countries, with an increase in water ponds. The normalized difference vegetation index showed that the riparian vegetation area increased by 36.9% during the monitoring period, indicating the stability of the valley floor.

Keywords: meandering, land use/cover, Landsat TM, migration, supervised classification.

Introduction

River meandering dynamics is an important indicator of environmental change related to climate changes and the scarcity of water resources in the lower Jordan River Basin. This seems to be dictated by the water conflict in the area, as water is a political issue within the riparian basin of the Jordan River (Beaumont, 1997; Barinava, et al., 2010; UN-ESCWA and BGR, 2013; Comair et al., 2012).

This has effects on water resources in the Dead Sea basin, and has caused a dramatic reduction in the Dead Sea water level by -39 meters since the 1950s (Al-Husban, 2014). Concomitantly, the surface water level of the Dead Sea areas has decreased from 1,050 km² to 625 km², and the volume has declined from 155 km³ to about 130 km³ (Klein, 1998; Magaritz et al., 1985; Al-Jayyousi, 2001; Jordan Valley Authority, 2016; Joan et al., 2001). The northern Dead Sea shoreline also retreated during the monitoring period by an 959.3 m up until 2016 (measured by ETM, 2016). The annual discharge of the lower Jordan River (LJR) has decreased from about 1,250 × 10⁶ m³ y⁻¹ to ca. 300 × 10⁶ m³ y⁻¹ due to water exploitation (Comair et al., 2012). Evidence from TM, ETM images and a topographic map from 1961 (base map) up until 2016 showed that the river was adjusting by two categories: (1) channel length and meandering; and (2) centreline migration. Many geomorphologic studies have been focused on changes in river characteristics of the channel patterns of adjustment over time, which are caused by changes in the river flow regime as a response to changes in flow reduction by dam construction and drought conditions (Brandt, 2000; Hooke, 1995; Hooke, 2006; Jiongxin et al., 2002; Magdaleno and Fernández-Yuste, 2011; Musselman, 2011; Nicoll and Hickin, 2010; Saleh et al., 2016; Brandt, 2000). With respect to land use/land cover (LULC)

change monitored in this study as a result of lack of water resources on the one hand and the vertical erosion of the Jordan River channel on the other, the normalized difference vegetation index (NDVI) was used to detect and investigate the changes that occurred in the study area affected by the morphological changes. The NDVI technique is widely used for monitoring environmental changes (USGS, 2010; Chavez and Mackinnon, 1994; Edward and Hicklin, 1984).

Study Area

The Lower Jordan River Basin (LJRB) has a total area of 18,500 km², of which 40% is located in Jordan, 37% in Israel, 10% in Syrian, 9% in the West Bank, and 4% in Lebanon. The total length of the lower Jordan River from Lebanon to its outlet (the Dead Sea) is some 250 km (Schattner, 1962). The length of the Lower Jordan Valley (LJV) from Tiberias Lake in the north to the Dead Sea in the south is 105 km. The LJV varies in width from more than 20 km near the northern shore of the Dead Sea to ca. 10 km along the northern course of the LJR, with a minimum of 4–5 km in its central part (Schattner, 1962). The LJR with the outflow from Tiberias Lake receives water from its main tributary, the Yarmouk River. The river then continues flowing south, forming the border between Israel and the West Bank to the west and Jordan to the east, and finally ends in the Dead Sea (FAO, 2009, Jordan River Basin). The Jordan Rift Valley is divided into three major parts: from its main sources at the foot of the Hermon up to Lake Hula; from Lake Hula to Lake Tiberias; and the LJV, from Tiberias lake to the Dead Sea, which is the section dealt with in this study (with an exclusion of about 17.3 km from the river exit from Tiberias Lake to the south because of the difficulty of distinguishing

and digitizing of the LJR in this region from the satellite images). The interest area lies between $31^{\circ}30'00''$ N - $31^{\circ}50'00''$ N latitude and $35^{\circ}30'00''$ E - $35^{\circ}40'00''$ E longitude (Fig. 1), with a total surface area of 2,792 km. The average annual precipitation in the basin is estimated to be 380 mm, although it varies all along the basin area. The Upper Basin, north of Tiberias Lake, has an annual precipitation of up to 400 mm, while the Lower Jordan Basin has an average annual precipitation rate of 100 mm only at its southern part. The largest part of the fertile land in the basin is located in Jordan and the West Bank, along the eastern and western banks of the Jordan River and the side wadies, in an area with an annual rainfall of less than 350 mm. The total area equipped for irrigation in the Jordan River Basin is estimated to be 32% in Jordan, 31% in Israel, 30% in Syria, 5% in the West Bank, and 2% in Lebanon. The Jordan River meanders along 215 km down to the Dead Sea (Schattner, 1962). Most of

the study area comprising 2,133.27 km² (76%) consists of the exposed area, and 584.6 km² (21%) is used for agriculture (according to the results of ETM analysis, 2016). Historically, the lower part of the Jordan River received about 1,070 MCM/year from Tiberias Lake (Sea of Galilee) and the Yarmouk River, and the LJR had an outflow into the Dead Sea of about 1,200–1,300 MCM/year (Jordan Valley Authority, 2016). But since the 1950s, the water has been diverted mainly by Israel, and the construction of many dams in Syria, in addition to existing dams (Unity Wahda, Wadi Arab, Shurabil Bin Hasna, King Talal, Karamah, Shueib, and Kafrein) constructed in the last 50 years in Jordan. The outflow into the Dead Sea is about 70–100 MCM/year (Hassan and Klein, 2002), which led to a decline in the Dead Sea level by -39m (Ministry of Water and Irrigation, 2016). The study area is covered with Holocene and Pleistocene non-cohesive geological formations. It consists mainly of a Zor unit in the narrow flood plain of

Fig. 1

The extent of the Lower Jordan River, from the mosaic of four topographic maps with a scale of 25,000, and the extracted LJR from the topographic map

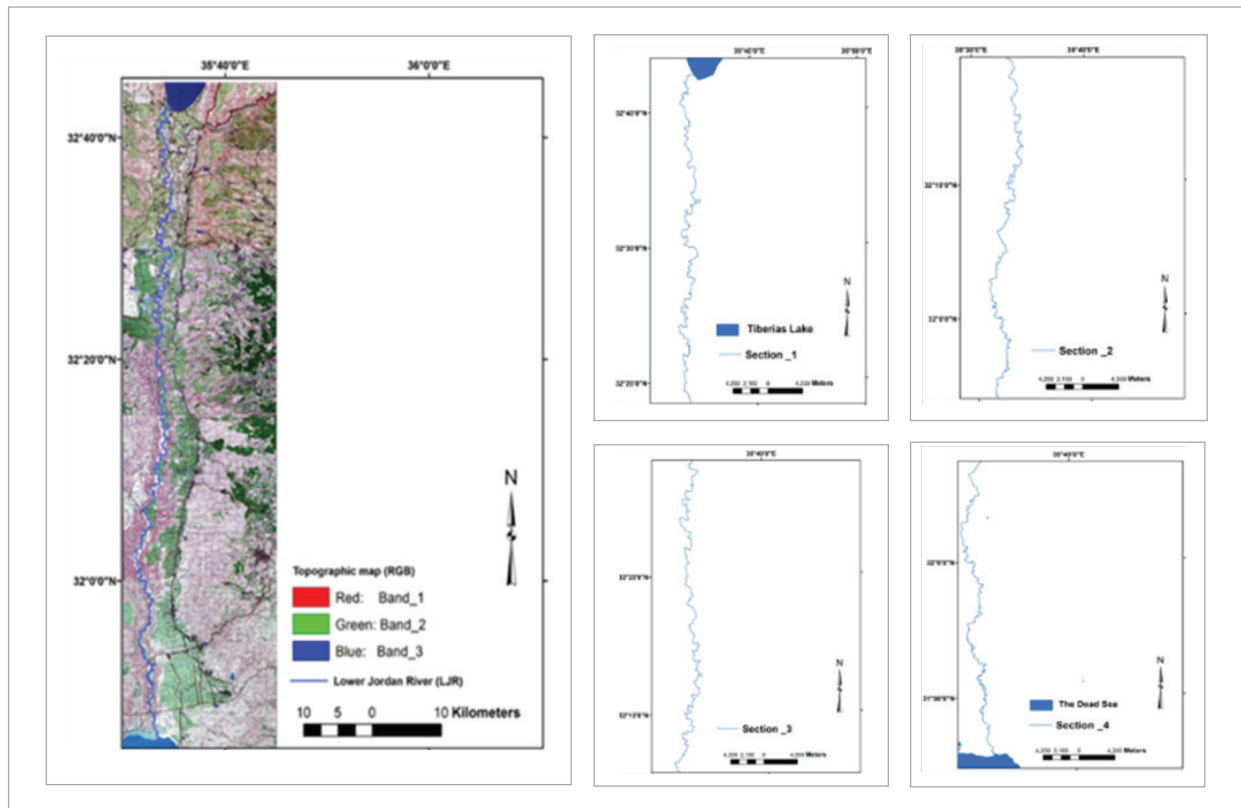
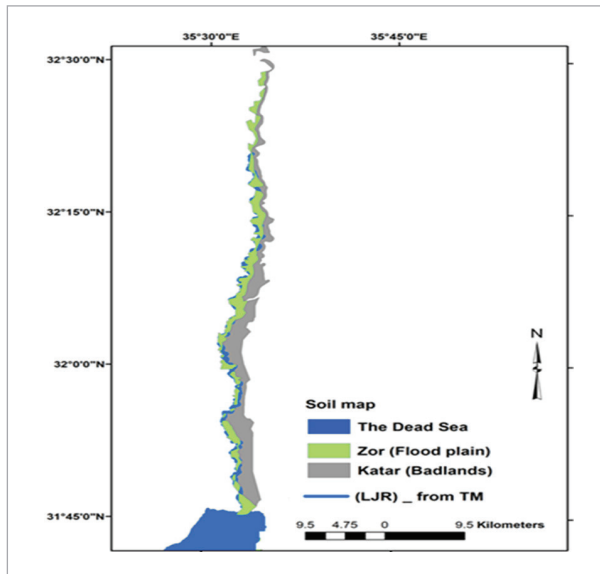


Fig. 2

Distribution of Katar and Zor along the LJR



the Jordan River, which extends from the junction of Yarmouk River–Jordan River in the north to the Dead Sea in the south (Ramadan and Auda, 1986; Bender, 1974), and a Katar or badland unit (Fig. 2). The dominant soil type is classified as fine, mixed, hyperthermic, with a deep family of brown to strong brown silty clay loam and alluvial gravels (Ministry of Agriculture, Jordan, 1995).

Data and Methodology

Data

Analysis of the river variables includes the channel length, meandering, centreline migration, as based on the topographic maps, TM images and DEM-derived from (SRTM) data. Details of the data are shown below.

The available four topographic maps covered the study area with a scale of 1: 25,000, generated by the Royal

Table 1

RMS error for the four TM plates covering the study area

Sheet (1) Al-Karamah	X map	Y map	RMS error
1	2	3	4
The editorial office of the journal - electronically	35.5001	31.747663	0.000368
	35.7494	31.748235	0.000368
	35.7499	31.998993	0.000325
	35.5018	31.998993	0.000343
	35.5018	31.998993	0.000320
Sheet (2) As Salt	35.7498	31.999222	0.000411
	35.7483	32.247732	0.000409
	35.5021	32.247732	0.000413
Sheet (3) Dier Abu Said	35.7505	32.249661	0.000312
	35.499	32.250423	0.000387
	35.749	32.497409	0.000326
Sheet (4) North Shona (Waqas)	35.5013	32.497409	0.000395
	35.5031	32.502829	0.000234
	35.7443	32.50554	0.000276
Sheet (4) North Shona (Waqas)	35.5004	32.74541	0.000280
	35.7471	32.74812	0.000432

Data Source for raw data: Royal Jordanian Geographical Center.

Table 2

Information of satellite images used in this paper

Satellite data	Acquisition date	Spatial resolution	Path and row	Pre-processing from the source
1	2	3	4	5
Landsat (5) TM	April/ 1984	30*30m	Path 174 Row 38	Georeferenced to UTM map projection, Zone 37 WGS 84ellepsoid
Landsat (7) ETM	April/ 2000	30*30m	Path 174 Row 38	Georeferenced to UTM map projection, Zone 37 WGS 84ellepsoid
Landsat (8) (OLI)	April/ 2016	30*30m	Path 174 Row 38	Georeferenced to UTM map projection, Zone 37 WGS 84ellepsoid

Jordanian Geographical Center (RJGC) covering the study area (Fig. 1). This map is considering the base map of the study area showing the dimensions of the meandering belt and the location of the channel. The TM maps were scanned, merged and mosaicked to have the same cell resolution 7.8 m and the coordinate system (Arc Toolbox, Data Management, Raster, and Mosaic; Al-husban, 2017). They were georectified using the Ge-referencing tools available in ARCGIS, and extracted by mask using Arc Toolbox and cartography tools (masking tools) (Table 1).

The digital elevation model (DEM) was derived from the shuttle radar topographic mission (SRTM) with a 30-meter ground resolution. The digital elevation model was used to analyze the topography of the channel and valley. Satellite images TM and ETM: three images were

acquired in April 1984, 2000 and 2016 (Table 2), available at the website <http://glovis.usgs.gov>. These images were georeferenced and rectified to the Jordan Transverse Mercator (JTM) Coordinate System using 1: 25,000 topographic maps.

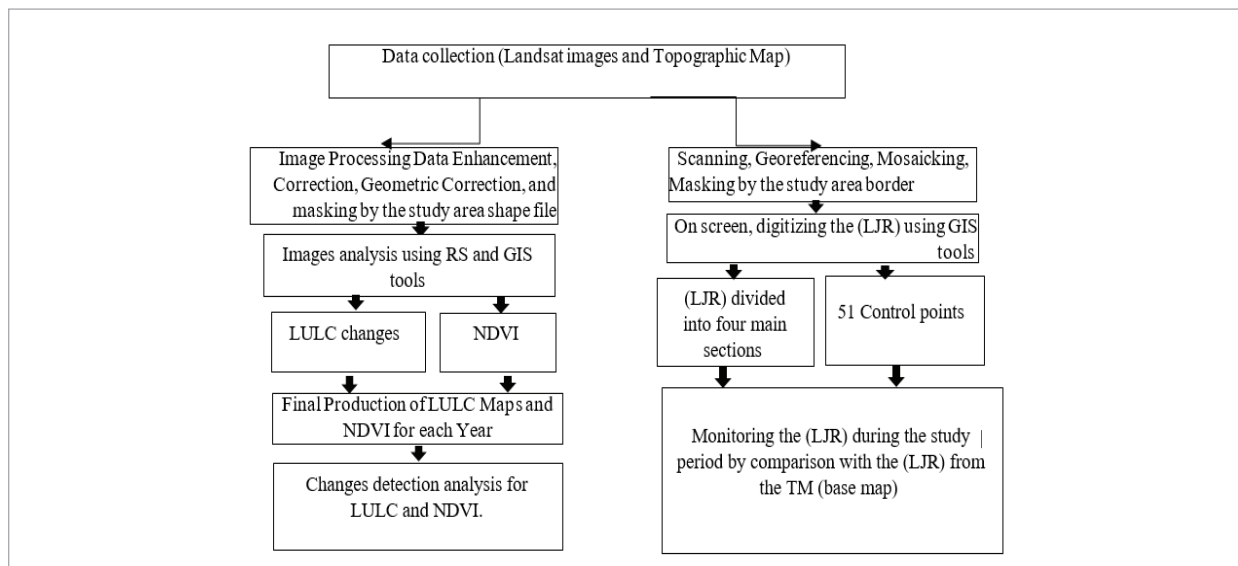
Methodology

To achieve the study goals we applied two main methodologies as illustrated in Fig. 3. The flowchart of the methodology is as follows.

Changes in the channel morphology. We assessed changes in channel length and meandering of the LJR

Fig. 3

Flowchart of the methodology



for each respective year by digitizing the river channel on screen. Then the study area was divided into four main sections in order to evaluate each of the variables (Table 4), the river polylines were overlaid (1961 (TM); 1984; 2000; 2016) to identify overall river channel changes (ARCGIS.V.10.4. using snapping tools).

Land Use/Cover assessment. The land-cover data for the monitoring period 1984–2016 were obtained from Landsat-5,7, and 8 multispectral imagery; spectral bands of all TM digital data (with the thermal bands excluded) were individually used as input for supervised classification purposes, with a spatial resolution of 30*30 m; all images were collected in April. ENVI5.8 was used for layer stacking. In total, four land use/cover classes were identified: 1) water bodies, 2) bare soil, 3) built-up area, and 4) irrigated area. Detailed definitions for these five categories and the relative percentage of each category are given in Table 5.

NDVI and image-differencing-generated image for the riparian vegetation. For monitoring the normalized difference vegetation index, it was calculated during the monitoring period using Eq. 1: $NDVI = \frac{(NIR - Red)}{(NIR + Red)}$, (AUG Signals, 2012; Al-Bakri et al., 2013; John et al., 1998), where Near Infra Red (NIR) is the band 4 for both 1984 TM and 2002 ETM images, and Red is the band 3 for both images 1984 and 2000. Near Infra Red is band 5 and Red is band 4 for 2016, while for land degradation monitoring and changes in riparian vegetation, an image-differencing method was adopted for pixel-by-pixel comparison and was performed on the NDVI-generated images of all dates. Image differencing was calculated using Eq. 2, later Image-Former Image, using GIS tools (Raster calculator).

Discussion and Results

Discussion

The changes in the study area due to the decrease of water discharge and the decline of the ultimate base level are as follows.

Active channel length (ACL) and elongation

The active channel length measured in 1961 from the TM, which is the base year, was 198.7 km, and it increased by 134 m between 1961–1984 and 300 m

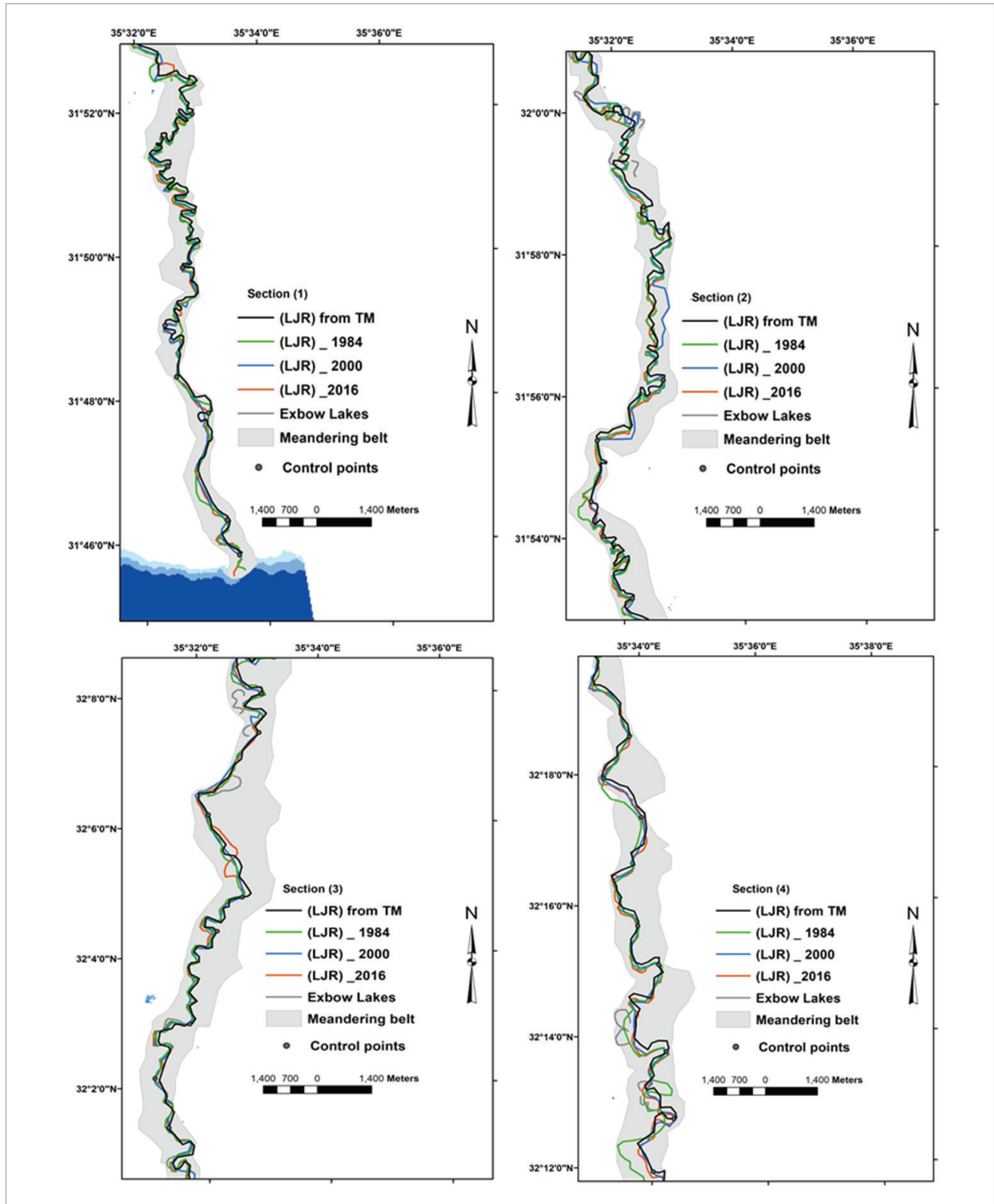
between 1961–2000 and up to 959.3 m during the monitoring period 1961–2016 (Fig. 4). The reason for this change is the decrease discharge and the decreasing of the river power in both vertical and lateral erosion. This led to an increase in the channel meandering from 1.8 to 2 and 2.04, respectively. The area of the active channel has decreased by 42% during the monitoring period. These changes in length and area form a type of channel adjustment (O'Connora et al., 2003; Yang, 1971; Chen and Duan, 2006).

Changes in channel meandering

The channel meandering explains the relationship between the length of the channel and the length of the valley (Eq. 3), $(P \text{ (sinuosity)} = LC/LV)$ (Nicholas et al., 2014). The channel could be considered as meandering if the length of meandering streams is about 1.5 times the valley length (Hooke, 1995). Meandering changes over time in different ways and directions. Over the last century, freely meandering channels have attracted a great deal of attention from morphologists (Schattner, 1962; Mehran et al., 2017; Muselman, 2011). The meandering channel was calculated in 51 channel segments and is presented in Table 4. The purpose is to determine the changes in the meandering level from 1961 to 2016. The measurements showed that there were changes in the mean channel meandering from 1.8 in 1961 to more than 2 in 2016. The meandering changes are classified as irregular patterns and the curved shape was common among the river meandering (Kolla, 2007). Fig. 4 and Table 4 show the river channel meandering and meander belt width, with insignificant changes during the study period. The meandering shows a pattern of adjustment for the reduction of water discharge, geological structure, and increasing the valley bed height due to sediment accumulation. Slope is key Factor that affect the meandering in different river basins (Leopold and Wolman, 1960; Yang, 1971). Meandering channels are sinuous single-thread channels that are typically found on low slopes and in fine-textured floodplain soils, silt and clay (Hassan and Micha, 2002). The rate of reduction in bank-full width depends on the geological controls surrounding the banks and represented by Holocene deposits. This covers all the study area including the ruggedness and high salinity badlands.

Fig. 4

LJR channel digitized on screen from a topographic map and for years 1984, 2000, and 2016 from the satellite imagery



In addition, there is a reduction of flow, which causes a reduction in stream power and security of peak flood. The river terraces develop as the Dead Sea level drops, the land around the Dead Sea is raised, and then the LJR has more work to do by vertical erosion to return to its equilibrium profile. In this case, the river returns to the youth stage (rejuvenation). The main causes of rejuvenation are uplift of the ground, lowering of the base level, and decrease in sediment load. Various landforms are formed by a reactivated channel process. A rejuvenated river will cut down into its original alluvial flood plain, which is then left as flat side terraces above the new level of the river. The new valley widens in time, forming a second flood plain within the first one, but at a lower level. If more uplift and rejuvenation occur, then a second set of terraces may form. Bended course is typical for areas with little slope, in lowland (Fig. 5) (Fan et al., 2006).

Active channel migration (centreline)

Many studies have been focused on the effect of changing water discharge, slope, and bed sediment on the mobility of channel by migration (Schattner, 1962;

Nicholas et al., 2014). Active channel centreline migration is related to the base map, and the site of the river mouth changing during the study period. Channel activity is measured by the rate and direction of migration towards the east and the west. In order to determine the channel migration rate and direction, 51 test locations were examined for the base topographic map for the year 1961. The results showed that the direction of active channel migration was concentrated towards the west, with the mean rate of channel centreline migration about 0.325 m/year. The position of the channel centreline fluctuated between the west and the east; but there is a general trend for the centre channel in 1984 towards the west, compared with the active channel in 2000. The measurement showed that the total migration towards the west is ca. 1,042 m, and 450 m east, while approximately 43 km represent a stable active channel. In 2016, the total channel migration was towards the eastern direction with a value of 463 m, and 1,616 m towards the north. The general trend of channel river migration in 2016 was towards the west. Fig. 3 shows the location of the active channel in relation to the base year of 1961.

Fig. 5

(A) The slope map of the study area, extracted from ASTER DEM with 30-m ground resolution. (B) The river mouth and the only cut-off of a meander labelled number (1) and the Dead Sea retreat during the monitoring period. (C) Distribution of the historical abandoned channel formations from Pleistocene to Holocene

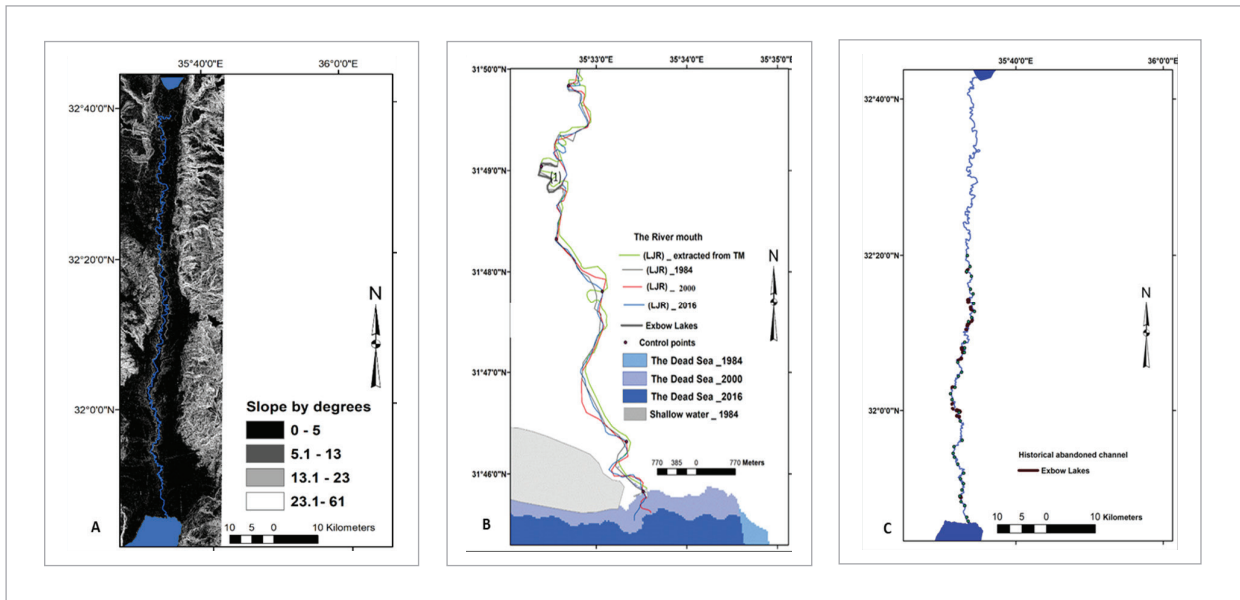


Table 3

Channel meandering and migration within the meandering belt

Control points	Meander (1984)	Description	Meander (2000)	Description	Meander (2016)	Description
1	2	3	4	5	6	7
1	1.6	Lateral movement (west)	1.5	Lateral movement (west)	1.5	Lateral movement (west)
2	1.6	No change	1.7	Lateral movement (west)	No change	Lateral movement (east)
3	1.4	No change	1.5	No change	1.5	No change
4	1.6	Lateral movement (west)	1.7	Lateral movement (west)	1.8	Lateral movement (west)
5	1.6	Lateral movement (west)	1.6	Lateral movement (west)	No change	Lateral movement (east)
6	1.5	No change	1.7	No change	1.7	No change
7	1.6	Lateral movement (west)	1.6	Lateral movement (west)	1.7	Lateral movement (west)
8	1.5	No change	1.6	Lateral movement (west)	1.7	Lateral movement (west)
9	1.6	Lateral movement (west)	1.7	Lateral movement (west)	1.8	Lateral movement (west)
10	1.6	No change	1.7	Lateral movement (west)	1.7	No change
11	1.5	No change	1.7	Lateral movement (west)	No change	Lateral movement (west)
12	1.7	Lateral movement (east)	No change	Lateral movement (east)	No change	Lateral movement (east)
13	1.8	No change	1.8	No change	No change	Lateral movement (west)
14	1.6	No change	1.8	Lateral movement (west)	No change	No change
15	1.7	No change	1.8	Lateral movement (west)	No change	Lateral movement (east)
16	1.6	No change	1.6	No change	1.7	Lateral movement (west)
17	1.7	No change	1.7	Lateral movement (east)	1.7	Lateral movement (east)
18	1.6	No change	1.6	Lateral movement (west)	1.7	Lateral movement (west)
19	1.6	No change	1.7	Lateral movement (east)	1.7	Lateral movement (east)
20	1.5	No change	1.7	Lateral movement (west)	No change	Lateral movement (west)
21	1.6	No change	1.6	No change	1.6	No change
22	1.5	Lateral movement (west)	1.6	Lateral movement (west)	No change	No change
23	1.5	No change	1.6	Lateral movement (west)	1.7	Lateral movement (east)
24	1.5	No change	1.5	No change	No change	No change
25	1.6	No change	1.7	Lateral movement (west)	No change	Lateral movement (west)
26	1.5	No change	No change	No change	No change	No change

Control points	Meander (1984)	Description	Meander (2000)	Description	Meander (2016)	Description
1	2	3	4	5	6	7
27	1.6	No change	1.6	Lateral movement (west)	1.7	Lateral movement (west)
28	1.5	No change	No change	No change	No change	No change
29	1.5	No change	No change	No change	No change	No change
30	1.5	No change	1.6	Lateral movement (west)	1.6	Lateral movement (west)
31	1.5	No change	1.6	Lateral movement (west)	1.6	No change
32	1.5	No change	No change	No change	No change	No change
33	1.4	No change	1.7	Lateral movement (west)	No change	No change
34	1.5	No change	1.6	Lateral movement (east)	1.7	Lateral movement (east)
35	1.6	No change	1.6	Lateral movement (east)	1.6	Lateral movement (east)
36	1.5	No change	1.6	Lateral movement (east)	1.6	Lateral movement (east)
37	1.5	No change	No change	No change	No change	No change
38	1.5	No change	1.6	Lateral movement (east)	1.7	Lateral movement (east)
39	1.6	No change	No change	No change	No change	No change
40	1.5	No change	1.6	Lateral movement (west)	1.6	Lateral movement (east)
41	1.5	No change	1.7	Lateral movement (east)	No change	Lateral movement (west)
42	1.5	No change	1.6	Lateral movement (east)	No change	No change
43	1.4	No change	1.6	Lateral movement (west)	No change	No change
44	1.6	No change	1.6	No change	No change	Lateral movement (east)
45	1.5	No change	1.6	Lateral movement (west)	Lateral movement (west)	Lateral movement (west)
46	1.5	No change	1.6	Lateral movement (east)	No change	Lateral movement (east)
47	1.6	No change	1.6	Lateral movement (west)	No change	Lateral movement (west)
48	1.5	No change	1.6	Lateral movement (east)	No change	No change
49	1.6	No change	No change	Lateral movement (east)	No change	No change
50	1.6	No change	No change	No change	No change	No change
51	1.5	No change	1.5	Lateral movement (east)	No change	No change

Centreline location in relation to the meander belt

In order to determine the position of the active channel centreline in relation to the meander belt centre, 51 points were chosen for the analysis. The measurements showed that there were significant changes and shifting (migration) in the active channel centreline towards the west and the east from the meander belt centre. In 1984, about 3.802 km of the total active channel located towards the west of the meander belt was mapped, while 1.432 km towards the east of the meander belt was measured. This means that the general trend for the active channel position was towards the west. In comparison with the year 2000, we found that 1.780 km were located in an easterly direction from the meander belt, and 2.947 km towards the western direction. Finally, in 2016, the total migration direction towards the west was 4.399 km, while the amount of migration direction towards the east was 1.242 km. This means that the general trend for the active channel heading position and migration was westward, the rest maintained relative stability. These dynamics of channel were due to the changes in water

discharge, and the retreat of the northern shoreline of the base level (Malik, 2005; Jiongxin et al., 2002).

Abandoned channel

One of the most common historical landscape developments in the flood plain of the LJR was the abandoned channel as a progressive increase in the number and area of mid-channel bars, accumulation of sediment, and neck cut-off. In comparison with 1984 and 2000, and 2016 with 1961 as a base year level, there were insignificant changes. But the phenomenon of abandoned channels caused by river meandering and the sedimentary formations was due to sedimentations from the Pleistocene to Holocene. Historical segments were measured with a total length of 33.48 km (see Table 4). During the monitoring period, the climate of the study area was characterized by decreasing rainfall and rarity of flood events (with the exception of 1991/1992) in the twentieth century. While the first section (Figs. 4, 6 and 7), especially near the river mouth, is within a distance of some 3 km from the northern Dead Sea

Table 4

Summary of the main variables of the LJR from the four sources north to south

Variables	First section	Second section	Third section	Fourth section
1	2	3	4	5
River length (km)	42.6708	46.814	55.67	53.54
Valley length (km)	23.8	27.531	27.212	26.212
Meandering	1.79	1.7	2.04	2.05
Mean meander belt width (m)	983	1024	1732	2.234
Number of islands in its course	5	7	13	3
Number of historical abandoned channels	6	13	11	15
Length of the historical abandoned channel (km)	6.98	13.76	8.45	4.29
Length of the abandoned channel during the study period (m)	No abandoned channel	726	No abandoned channel	No abandoned channel
Migration rate (m/per/y)	0.1	0.1	0.50	0.6
Dominant migration direction	towards east	towards east	towards west	towards west

shoreline cut-off of a meander, the only cutoff of a meander numbered 1 in Fig. 6 turned to an abandoned channel, with a length of 726 m during the monitoring period.

LULC changes

To map changes that occurred between the three dates, 6 spectral bands of both TM digital data were individually used as input for a supervised classification purpose. Supervised classification was applied. Maximum likelihood algorithm used for land use/cover mapping from Landsat images, depending upon 50 training points used as signature file for the

the (LULC) from google earth. (Fig. 6). Fieldwork in the study area is not possible practically in the valley floor because the river course forms the border between Jordan and Israel. The images were acquired in the same season in order to minimize the impacts of seasonal differences of vegetation. A maximum likelihood algorithm was used for land use/cover mapping from Landsat images (Menzel et al., 2009; Wood et al., 1992; Hossain et al., 2016). In this study, four land-cover classes could be identified. These are built-up area, agricultural area, water, and exposed area (Fig. 6). Definitions of these four categories of land use/cover are summarized in Table 5.

Fig. 6

(A, B) Colour composite image of Landsat TM 5 1984 and 2000 bands 3, 2, and 1 exposed through the blue, green and red filters and the LULC, respectively. (C) Colour composite image of Landsat 8 2016 bands 4, 3, and 2 exposed through the blue, green and red filters, respectively, and the LULC classification map

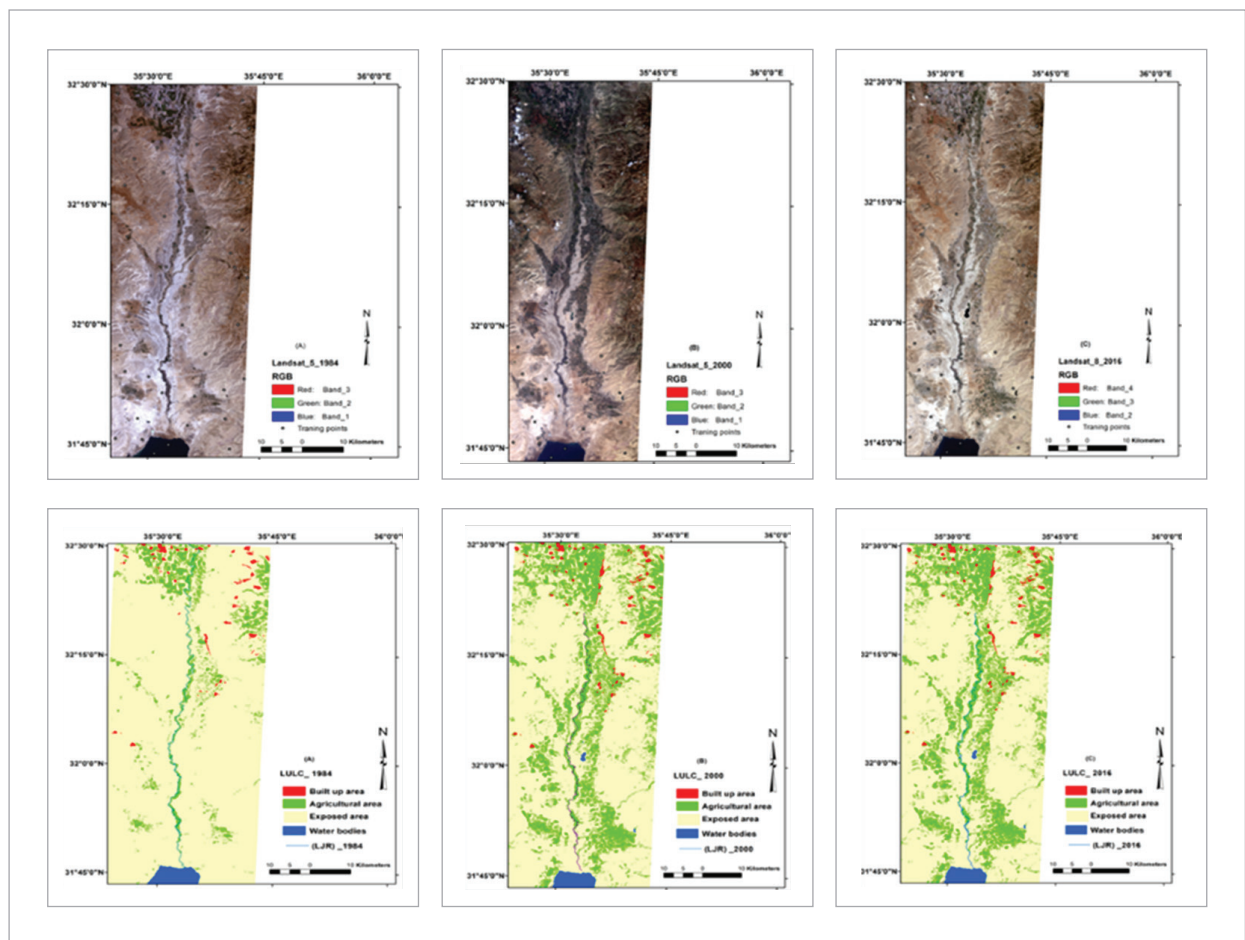


Table 5

Land use and land cover classes and definitions

Land/Use/Cover	Definitions
1	2
Built-up area	Construction materials, asphalt, commercial and industrial buildings, residential single/multiple houses, parking lots, highways, local roads.
Agricultural area	Irrigated area, rain fed area, riparian vegetation
Water bodies	The Dead Sea, Jordan River channel, irrigated ponds, and fishponds, farms and dams.
Exposed area	Newly exposed area (salty area), bare rock areas, gravels, stones and boulder areas, badlands, bare soils areas.

Table 6

Land use and land cover classes and definitions

Year	1948	2000		2016		Changes (%)		
Class	Area (km ²)	Percentage (%)	Area (km ²)	Percentage (%)	Area (km ²)	Percentage (%)	1984–2000	2000–2016
1	2	3	4	5	6	7	8	9
Built Up area	24	0.859	28	1.001	35.68	1.28	+0.142	+0.279
Agricultural area	189	6.76	202	7.25	584.6	20.94	+0.49	+13.69
Water	43	1.54	42	1.51	38.02	1.36	-0.03	-0.15
Exposed area	2,536	90.83	2519	90.23	2,133.27	76.40	-0.6	-13.83
Total	2,792	100	2791	1000	2,791.57	100%		

NDVI for riparian vegetation and image-differencing generated image

NDVI for riparian vegetation was generated for the three dates using Eq.1. Analysis of the NDVI images showed that the mean values of this index were low, reflecting water scarcity in the study area. The mean NDVI value 0.54. (Fig. 7) showed that most of the study area was characterized by high NDVI values ranging from 0.4 to 0.7, and 0.3. These results due to the stability of the channel and low amounts of the river discharge are the basic factors (Edward and Hicklin, 1984; Muller, 1995).

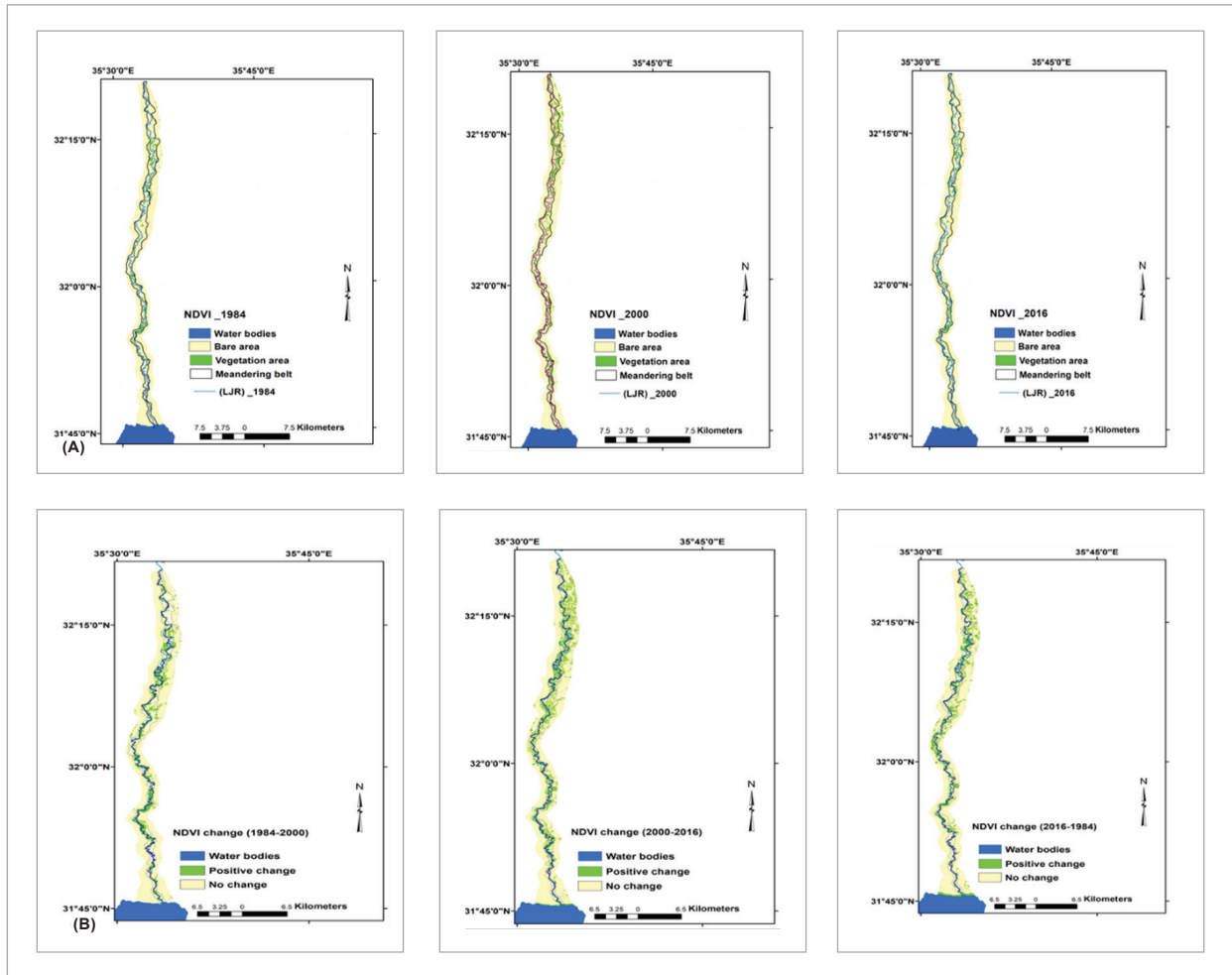
Monitoring NDVI image differencing

An image-differencing method was adopted for pixel-by-pixel comparison and was performed on the

NDVI-generated images of the three dates. The statistical results of the difference image results (refer to Tables 3 and 4) showed that NDVI values increased. NDVI value variations are presented in Fig. 7. The lowest values were found on the less vegetated soils, presumably because of reflection of the high salty area near the LJR mouth. Within the study area (upstream) along the entire bank, it was found that river banks with NDVI values of 0.45 or less were mostly eroded and banks with NDVI values of more than 0.45 were not eroded or almost stable. This means that the river is migrated at low biomass vegetated areas but not at high biomass vegetated areas, as high NDVI value represents vegetation of high biomass both above and below the ground. This study used only one vegetation index NDVI and a pixel of Landsat image that covers 30 m x 30 m ground area and represents one NDVI value (Paul and Schmidt,

Fig. 7

(A) NDVI at threshold values 0.2 for 1984, 2000 and 2016, respectively. (B) NDVI images differencing for 1984, 2000 and 2016, respectively



2002). Consequently, vegetation of a high NDVI will give comparatively high bank stability through dense root networks under the ground that affects bank migration as well as morph-dynamic activity.

Accuracy Assessment

Accuracy assessment is necessary for testing the accuracy of the result classes from the classification images. There are several methods of performing an accuracy assessment, such as the overall accuracy and the Kappa coefficient (Congalton, 1991). In order to obtain the confusion matrix, a random sampling was carried out. The columns of the matrix represent

the reference data, while the rows indicate the classes generated from the classification process. The Kappa coefficient is one of the most popular measures for addressing the difference between actual agreement and chance agreement (Congalton and Green, 1999; Booth and Oldfield, 1989). The Kappa coefficient of agreement was computed as Eq. 4

$$\hat{k} = \frac{N \sum_{i=1}^r X_{ii} - \sum_{i=1}^r (X_{i+} \times X_{+i})}{N^2 - \sum_{i=1}^r (X_{i+} \times X_{+i})}$$

Where: *r* is the number of rows in the confusion matrix;

Table 7

NDVI value and image differencing according to the monitoring period

Year	Minimum value	Maximum value	Riparian vegetation (%)	Riparian vegetation changed between 1984–2000	Riparian vegetation changed between 2000–2016	Riparian vegetation changed between 1984–2016
1	2	3	4	5	6	7
1984	-0.48	0.68	13.4	+16.8	+20.1	+36.9
2000	-0.45	0.60	30.2			
2016	-0.48	0.61	50.3			

Table 8

Confusion matrix of the signatures derived from supervised training, ETM 2016

Reference data						
Classified data	Built-up area	Agricultural area	Exposed area	Water bodies	Row total	User accuracy (%)
1	2	3	4	5	6	7
Built-up area	3	1	0	0	4	0.75
Agricultural area	1	10	1	0	12	0.91
Exposed area	0	0	31	0	31	0.94
Water bodies	0	0	1	2	3	1.00
Column total	4	11	33	2	50	89.96
Producer Accuracy (%)	0.75	0.83	1.00	0.67	81.25	
Producer Accuracy (%)	81.25					Overall Kappa Accuracy (%) 85.605

X_{ij} is the number of observation in row and column i ;
 X_{j-} is the total number of observation in column i ;

N is the total number of observations included in the matrix.

Accuracy assessment is presented in Table 4. Both user and producer accuracies were found to be between percentages 81.25 and 89.96 for the 2016 image. Also, overall classification accuracy and Kappa coefficient statistics were found to be at a percentage of 85.605.

Results

The LJR changes that were recorded over the monitoring period caused by the low reduction of water flow, rare flood events and the ultimate base level decline by -39 m resulted in decreasing the active channel by 42% during the monitoring period. The active channel length measured in 1961 from the TM, which is the base year, was 198.7 km, and it was increased by 134 m in the period 1961–1984 and by

300 m in the period 1961–2000 and up to 959.3 m during the monitoring period 1961–2016. The only cut-off of a meander numbered (1) in Fig. 5 turned to an abandoned channel, with a length of 726 m during the monitoring period. The width of the meander belt decreased in mean from 11.6 km in historical time to 935.3085 m during the study period. The direction of active channel migration is concentrated towards the west, with the mean rate of channel centreline migration of 0.325 m/year. There was expansion of the land use for the built-up area by +0.279 and agricultural area by +13.69, while there was a decrease in water by –0.15 and –13.83 for the exposed area.

References

- Al-Jayyousi, O., (2001), Jordan Valley Improvement Project Phase A-Report 2. The Hashemite Kingdom of Jordan, Ministry of Water and Irrigation, Jordan Valley authority, February 2001.
- Al-Husban, Y., (2014), Monitoring the Geomorphological Characteristics of the Lower Zarqa River Changes in Jordan, during the Time Period from 1963 to 2011, *International Journal of Applied Environmental Sciences*, 9, (2) (2014), 153-164.
- Al-husban, Y., (2017), Comparison of Accuracy of Two Global DEMs, and the Extracted DEM from the Topographic Map of the Tafilah Governorate, *Journal of Earth Science and Engineering* 7, 230-241. <https://doi.org/10.17265/2159-581X/2017.04.004>
- Barinava, S., Tavassi, M., Glassman, H. and Nevo, E. (2010), Algal indication of pollution in the lower Jordan River, Israel, *Applied Ecology and Environment Research* 8 (1): 19-38. https://doi.org/10.15666/aer/0801_019038
- Beaumont, P., (1997), Dividing the Waters of the River Jordan: An Analysis of the 1994 Israel-Jordan Peace Treaty. *Water Resources Development*, Vol. 13, No. 3, 415-424. <https://doi.org/10.1080/07900629749764>
- Bender, F., (1974), *Geology of Jordan (1968, 1974)*, Natural Resources Authority and German Geological Mission in Jordan, Hanover, Germany.
- Brandt, S.A., (2000), Classification of geomorphological effects-downstream of dams, *Catena* 40, 375–401. [https://doi.org/10.1016/S0341-8162\(00\)00093-X](https://doi.org/10.1016/S0341-8162(00)00093-X)
- Chavez, P.S., Jr., and MacKinnon, D., (1994), Automatic detection of vegetation changes in the southwestern United State using remotely sensed images.
- Chen, D., Duan, J.G., (2006), modelling width adjustment in me-

Riparian vegetation increased by +36.9% as a result of active channel stability.

Conclusions

The main findings of the analysis showed that most of the Lower Jordan River is characterized by stability due to the shortage of water discharge by controlling the water in dams and canals and expansion of the land use; this stability is evidenced by increased riparian vegetation, while the most dynamic and changing part is the river mouth, where the Dead Sea is retreating.

andering channels, *Journal of Hydrology* 321, 59–76. <https://doi.org/10.1016/j.jhydrol.2005.07.034>

Congalton, R. G. and Green, K. 2008. *Assessing the Accuracy of Remotely Sensed Data: Principles and Practices*, Second Edition. CRC Press. <https://doi.org/10.1201/9781420055139>

Comair, G.F., McKinney D.C., and Siegel, D., (2012), Hydrology of the Jordan River Basin: Watershed Delineation, *Water Resources Management* DOI 10.1007/s11269-012-0144-8. p 1-13. <https://doi.org/10.1007/s11269-012-0144-8>

Edward, and Hicklin, (1984), Vegetation and River Channel dynamics, *Canadian Geographer*. XXVIII. 2, 112.

Fan, H, Huang H., Thomas Q., and Zeng, Kairong Wang, K.W., (2006), River mouth bar formation, riverbed aggradation and channel migration in the modern Huanghe (Yellow) River delta, *China Geomorphology* 74, 124– 136. <https://doi.org/10.1016/j.geomorph.2005.08.015>

Hashemite Kingdam of Jordan, Ministry of Agriculture, commission of the European contract, National Soil Map, and land use project (The soil of Jordan), level 1, Vol.2, Main Report.(1994). p. 183.

Hassan, A., Micha, K., (2002), fluvial adjustment of the Lower Jordan River to a drop in the Dead Sea level, *Geomorphology* 45, 21–33. [https://doi.org/10.1016/S0169-555X\(01\)00187-8](https://doi.org/10.1016/S0169-555X(01)00187-8)

Hooke J.M., (1995), River channel adjustment to meander cut-offs on the River Bollin and River Dane, northwest England, *Geomorphology* 14, 235-253. [https://doi.org/10.1016/0169-555X\(95\)00110-Q](https://doi.org/10.1016/0169-555X(95)00110-Q)

Hooke, J., (2006), Hydromorphological adjustment in meandering river systems and the role of flood events, *Sediment Dynamics and the Hydromorphology of Fluvial Systems* (Pro-

- ceedings of a symposium held in Dundee, UK . IAHS Publ. 306.
- International UNION for conservation of nature –regional office for West Asia, Sustainable dryland landscapes management rangeland in Jordan, 2015, 1-34.
- Jiongxin, Xu, Michiel, C.J., Damen & Robert A. van Zuidam, (2002), River sedimentation and channel adjustment of the lower Yellow River as influenced by low discharges and seasonal channel dry-ups, *Geomorphology* 43, 151–164. pP.152.
- Jordan Valley Authority (JVA), (2016), under the Ministry of, Water and Irrigation (MWI) Water Authority of Jordan (WAJ).
- Klein, M., (1998), Water balance of the Upper Jordan River basin. *Water Int.* 23, 244– 248. <https://doi.org/10.1080/02508069808686778>
- Kolla V., (2007), a review of sinuous channel avulsion patterns in some major deep-sea fans and factors controlling them, *Marine and Petroleum Geology* 24, 450–469. <https://doi.org/10.1016/j.marpetgeo.2007.01.004>
- Leopold, L.B., Wolman, M.G. (1960), River meanders. *Bull Geol-Soc Am* 71:769–794. [https://doi.org/10.1130/0016-7606\(1960\)71\[769:RM\]2.0.CO;2](https://doi.org/10.1130/0016-7606(1960)71[769:RM]2.0.CO;2)
- Magdaleno F. Fernández-Yuste j.A. (2011), Meander dynamics in a changing river corridor, *Geomorphology* 130, 197–207. <https://doi.org/10.1016/j.geomorph.2011.03.016>
- Magaritz, A.M., and Neev, D., (1985), Dead Sea and Lake Lisan levels in the last 30,000 years: a preliminary report. *Report Geol. Survey of Israel* No. 29/85, pp 18.
- Malik I., (2005), Rates of lateral channel migration along the Mala Panew River (southern Poland) based on dating riparian trees and Coarse Woody Debris, *Dendrochronologia* 23, 29–38. <https://doi.org/10.1016/j.dendro.2005.07.004>
- Mehran Maghsoudi, M., Seyyed Mohammad Zamanzadeh, Mojtaba Yamani, Abdolhossein Hajizadeh, (2017), Morphometric Assessment of Meandering River in Arid Region Using Improvement Model (Case Study: Maroon River), *Journal of Water Resource and Protection*, 2017, 9, 358-377. <https://doi.org/10.4236/jwarp.2017.94024>
- Musselman.Z.A., (2011), The localized role of base level lowering on channel adjustment of tributary streams in the Trinity River basin downstream of Livingston Dam, Texas, USA, *Geomorphology*, 128, 42-56. <https://doi.org/10.1016/j.geomorph.2010.12.021>
- Menzel, L., Koch J., Onigkeit J., and Schaldach R. (2009), Modelling the effects of land-use and land-cover change on water availability in the Jordan River region, *Advances in Geosciences*, 21, 73–80. <https://doi.org/10.5194/adgeo-21-73-2009>
- Morin, E., et al., (2009), Flash Flood Prediction in the Dead Sea Region Utilizing Radar Rainfall Data. *Journal of Dead-Sea and Arava Research*, 1, 1066-1076.
- Ministry of Agriculture, Jordan, MOA., (1995), The soils of Jordan: Level 2 (Semi Detailed Studies), Report of the National Soil Map and Land Use Project, Vol. 3, Ministry of Agriculture, Amman, Jordan.
- Nicoll.T., J.and Hickin.E.J., (2010), Planform geometry and channel migration of confined meandering rivers on the Canadian prairies, *Geomorphology* 116, 37– 47. <https://doi.org/10.1016/j.geomorph.2009.10.005>
- Nicholas T., Legg and Patricia L., Olson, (2014), Channel Migration Processes and Patterns in Western Washington A Synthesis for Floodplain Management and Restoration, August Publication no.14-06-028.
- O’Connora, J.E., Myrtle A. Jones, Tana L. Haluska, (2003), Flood plain and channel dynamics of the Quinault and Queets Rivers, Washington, USA, *Geomorphology* 51, 31–59. [https://doi.org/10.1016/S0169-555X\(02\)00324-0](https://doi.org/10.1016/S0169-555X(02)00324-0)
- Paul, E.G., Schmidt, John C., (2002), Stream flow regulation and multi-level flood plain formation: channel narrowing on the aggrading Green River in the eastern Uinta Mountains, Colorado and Utah, *Geomorphology*, 4 4, 337–360.
- Ramadan H., Auda S., (1986), Geomorphologic Katar around the lower part of the Zarqa River, *Human and Social Sciences*, 13(7), 23-61.
- Saleh Yousef, S., Reza, H., Pourghasemi, x.x., Hooke, J., Oldrich, N., and Kidová, A., (2016), Changes in morphometric meander parameters identified on the Karoon River, Iran, using remote sensing data, *Geomorphology*, 271, 55-64. <https://doi.org/10.1016/j.geomorph.2016.07.034>
- Schattner, I., (1962), the Lower Jordan Valley. *Scr. Hierosolymitana* XI, 123 pp. Jerusalem, Magnes Press, the Hebrew University.
- Smith, R.B., (2012), Introduction to Remote Sensing. Lecture Notes. <https://fortress.wa.gov/ecy/publications/SummaryPages/1406028.html>
- US Geological Survey (1998) Overview of Middle East Water Resources: Water Resources of Palestinian, Jordanian and Israeli Interest. Water Data Bank Project, Executive Action Team, New York, 41.
- UN-ESCWA and BGR (United Nations Economic and Social Commission for Western Asia; PART I Jordan River Basin, Bundesanstalt für Geowissenschaften und Rohstoffe, (2013), Inventory of Shared Water Resources in Western Asia. Beirut. pp. 170-220.
- Wood, L.J., Etheridge, F.G., Schumm, S.A., (1992), the effects of rate of base-level fluctuation on coastal-plains shelf, and slope depositional systems: an experimental approach. *Spec. Publ. Int.Assoc. Sedimentology*. 18.
- Yang, C.T., (1971), on river meanders. *Journal of Hydrology* 13(3):231–253. [https://doi.org/10.1016/0022-1694\(71\)90226-5](https://doi.org/10.1016/0022-1694(71)90226-5)
- Žemės dangos pokyčių aptikimas Žemutinėje Jordano upėje, 1984–2016 m., Naudojant GIS ir RS

Žemės dangos pokyčių aptikimas Žemutinėje Jordano upėje, 1984-2016 m., naudojant GIS ir RS

Yusra Al-husban

Jordanijos universitetas, Amanas, Jordanija

Šio tyrimo tikslas - stebėti ir analizuoti žemės dangos pasikeitimus (LULC), kuriuos sukelia didelis mažesnio Jordano upės (LJR) vandens srauto sumažėjimas dėl klimato sąlygų Jordanijoje viršutinėje Jordano upės baseino dalyje. Dėl šių aplinkybių monitoringo laikotarpiu Negyvosios jūros lygis išaugo vertikaliu atstumu -39 m. Tai lėmė vandens išteklių trūkumą, pokyčius, darančius įtaką upės geomorfologijai, taip pat vegetatyvinei teritorijai ir pakrančių augmenijos erdviniam pasiskirstymui LJR. Šie pokyčiai buvo išnagrinėti naudojant Landsat TM, ETM, visus vaizdus, kurie buvo gauti 1984 m., 2000 m. Ir 2016 m. Rūgpiūtį, o bazinis žemėlapis buvo naudojamas topografinis žemėlapis (TM). Daugiasluoksniai vaizdai buvo geometriniai ir radijo ryšio metrinis kalibravimas vienas kitam ir naudojami kaip įvedimo automatinio keitimo nustatymo procedūra. Išaiškinimo rezultatai parodė, kad per stebėsenos laikotarpį aktyviojo kanalo ilgis buvo apie 741,8 m, nes Negyvosios jūros pakrančių atkūrimas ir apie 2,65 km, kuriuos sukėlė bangavimas. Migracijos lygių kryptis nukreipta į vakarus ir rytus, dominuojanti kryptimi į vakarus, o metinė vidutinė migracija į vakarus ir rytus buvo 0,325 m, o tyrimo laikotarpiu bendra šoninė migracija siekė tik 17,875 m abiem kryptimis - vakarai ir rytai. Upių srovė išaugo nuo 1,8 m iki 2,1 m. Atsižvelgiant į LULC, skirtumų vaizdas parodė, kad nuo 1984 iki 2016 m. pastebimi teigiami žalios vegetacijos pokyčiai; tai yra dėl vandens kanalų ir užtvankų išplėtimo visose pakrančių šalyse, padidinus vandens tvenkinius. Normalizuoto skirtumo vegetacijos indeksas parodė, kad stebėjimo laikotarpiu pakrančių augmenijos plotas padidėjo 36,9%, o tai rodo slėnio žemės stabilumą.

Raktiniai žodžiai: žemės naudojimas / danga, "Landsat TM", migracija.

Gauta:
2018 m. birželis

Priimta spaudai:
2018 m. rugsėjis